Lateral stability of long precast concrete beams

T. J. Stratford, BA, BEng, and C. J. Burgoyne, BA, MSc, CEng, MICE

Proc. Instn Civ. Engrs Structs & Bldgs, 1999, **124**, May, 169–180

Paper 11809

Written discussion closes 27 August 1999

Modern precast concrete bridge beams are becoming increasingly long and slender, making them more susceptible to buckling failure. This paper shows that once the beam is positioned in the structure, buckling failure is unlikely to occur. However, during lifting, a beam is less stable. A theoretical background is presented which will allow design procedures to be derived.

Keywords: beams & girders; design methods & aims

Notation

a	distance of yoke attachment point from end of beam
b	distance of yoke attachment point from centre of beam
d	beam depth
E	Young's modulus of concrete
G	shear modulus of concrete
h	height of yoke to cable attachment points above the centroid of the beam
I_x	second moment of area about the beam section's major axis
I_y	second moment of area about the beam section's minor axis
J	St Venant's torsion constant for beam section
k	describes support condition for lateral–torsional buckling
L	length of beam
$v(x)$	lateral deflection measured in the minor-axis direction (which rotates with θ)
v_0	initial lateral imperfection
v_{ms}	midspan lateral deflection along minor axis of beam
w	self-weight of beam per unit length
w_{cr}	critical self-weight of beam to cause buckling per unit length
x	distance along beam, measured from the yoke attachment point
$y(x)$	lateral deflection measured along a fixed axis
y_0	initial lateral imperfection
y_b	distance of bottom fibre of beam below centroid of beam
y_{ms}	midspan lateral deflection measured along an axis fixed relative to the supports
y_{sc}	distance of shear centre below centroid of beam
α	cable inclination angle above the horizontal
β	yoke inclination angle above the horizontal
Γ	warping constant for beam section
δ_0	magnitude of initial lateral imperfection
η	rotation of beam
θ	roll angle: rigid-body rotation about the beam's axis
$\delta\theta$	twist about beam axis
κ_{ms}	midspan curvature about minor axis

Introduction

Precast, prestressed concrete beams are widely used in construction projects where speed and ease of erection are important. A number of different bridge beam sections are available, reflecting the range of applications for which they are intended. The development of these standard sections has primarily followed the industry's demand for increasing spans—from the early inverted T- and I-sections of the 1950s,[1] through the M-beam[2] (introduced in the mid-1960s), to the modern Y-beam[3] (introduced in 1991). The development of the Super-Y (SY) beam[4] in 1992 allows the construction of bridges with spans of up to 40 m, for example in motorway widening schemes. In the USA 45 m long beams are commonly used.[5] Figure 1 compares the T-10, M-10, Y-8 and SY-6 beam sections; these are the largest beams in their respective ranges.

2. A consequence of increasing the span has been increased weight, so that the longest beams are now limited by transportation considerations. To maximize the span range, the weight of modern beams has been kept to a minimum by reducing the width of the flanges, resulting in lower minor-axis and torsional stiffnesses compared to older sections. But the increased weight means that only a single beam can be carried on a truck, whereas two or more have been carried in the past, which allowed them to be cross-braced to each other. It has, hitherto, been the practice to pay little attention to buckling considerations, since concrete beams have always been considered to have a large reserve of minor-axis stiffness; current codes include only very crude stability checks. It will be shown below that beams are now available which, although they are stable if built and handled properly, are in the region where an understanding of stability phenomena, in particular imperfection sensitivity, is becoming important. Any further increase in span (beyond 40 m) or slenderness will mean that stability will definitely become a significant design constraint.

T. J. Stratford, Department of Engineering, University of Cambridge

C. J. Burgoyne, Department of Engineering, University of Cambridge

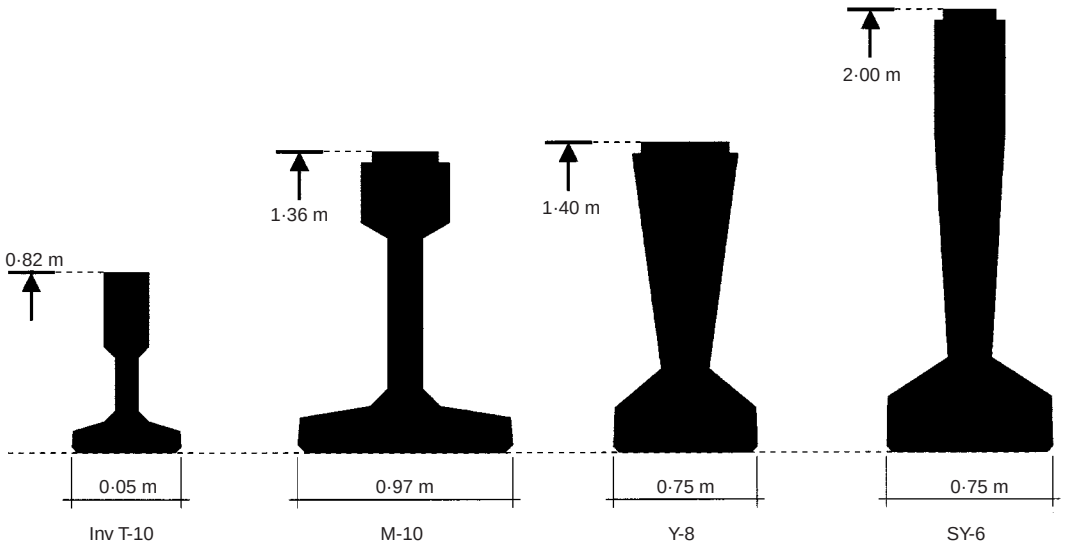

Fig. 1. The development of precast beam sections: the T-10, M-10, Y-8 and SY-6 beams

3. Stability checks for steel beams have always been important and there is an enormous literature on the subject.[6–9] But there are important differences when considering concrete beams: self-weight is much more significant, their torsional stiffness is higher in comparison with their minor-axis stiffness, and the design of the prestress precludes supporting them at positions very far from the ends. Thus the temporary conditions, under self-weight loading, are much more important than the permanent loaded state, where the top slab acts to prevent buckling.

4. During their use precast beams are handled in a variety of ways. They must be transported from the precast yard to the construction site and may need to be lifted as many as four times between the casting bed and their final position within the bridge.

5. Three important stages can be identified in this process (Figs 2, 3, 4):

- lifting
- transportation
- placement in structure (or in temporary storage).

6. In recent years there have been a number of failures of modern slender beams, which have led to increased concern about stability considerations. Examples include the collapse of a 37 m long bridge beam in Bernay (France) while being prestressed[10] and the toppling of a 30 m long Y-beam in Northumberland due to inadequate support.[11] While these failures may not have been due directly to stability problems, the relative ease with which the beams could be toppled drew attention to the overall stability problem. This paper draws together

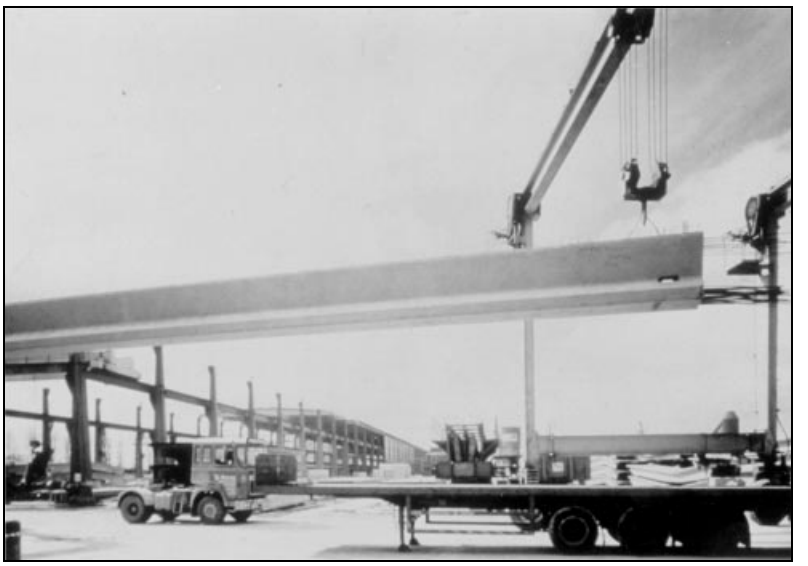

Fig. 2. A Y-beam being lifted in a storage yard

Fig. 3. Transportation of a pair of precast beams by road

the relevant literature and theory regarding the stability of precast concrete beams, and produces design charts. A companion paper[12] presents methods which can be used by designers to check the stability of projected beam sections.

Support conditions

7. In each stage of a beam's use it is supported in a different way, and hence the stability of the beam will require several different assessments. Figure 5 shows how these support conditions can be modelled for analysis and defines the parameters associated with the models.

Simply supported beam

8. The beam is simply supported at its ends, with no overhangs. The support is assumed to be at the soffit level (as shown in Fig. 5(a)) and is assumed to allow rotation about the major and minor axes, but to prevent axial rotation and deflection. More complex support conditions could be considered, but they are unlikely to be used with standard precast beams; they would need to be analysed as special cases.

9. There is a potential subsidiary problem, in which the beam can topple sideways if it is supported on rotationally flexible bearings which allow significant minor-axis rotation. This analysis will be described elsewhere.[13]

Transport-supported beam

10. Beams are commonly transported by road, where they span between a tractor unit and a trailer (Fig. 6). The supports at either end of the beam comprise a turntable (to allow cornering) and a roller (to allow for change in slope, such as when driving up a ramp). Various arrangements are possible, but the normal configuration is that on the trailer unit the roller is above the turntable and rotates with the beam. However, on the tractor unit the roller is below the turntable and hence can rotate relative to the beam. When extreme corners (such as roundabouts) are taken, the roller on the tractor can rotate so that it is in line with the beam, giving no restraint to axial rotation. As beams get longer, such extreme geometries become more likely, and should be taken into account in design.

11. This represents the most extreme support condition during transportation. The beam can be modelled as simply supported at one end (where axial rotation is restrained) and resting on a ball or pin at the other end, which prevents deflection but allows rotation (Fig. 5(b)). Both supports are at the soffit level. This model will be referred to as 'transport-supported' in the subsequent analysis.

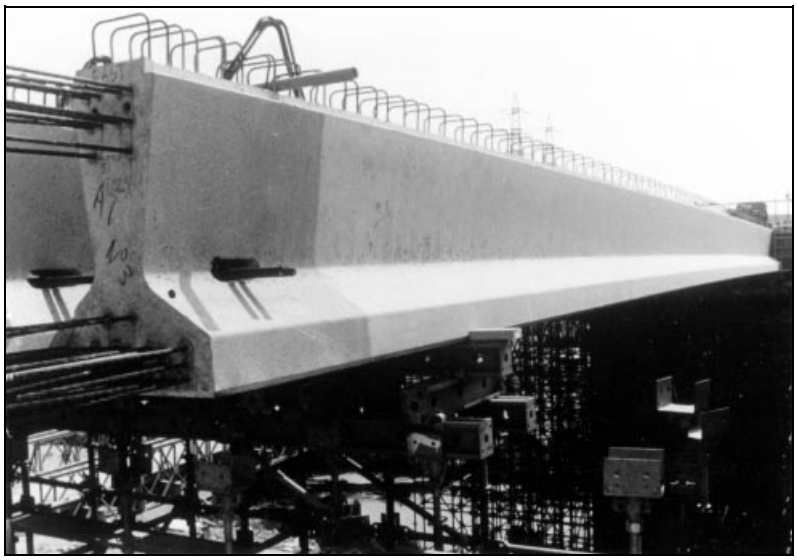

Fig. 4. A Y-beam on temporary simple supports

Hanging beam

12. When a beam is lifted on site, it typically hangs from two inclined cables on a single crane, while in the precasting factory it is invariably lifted using vertical cables supported from two cranes. In either case these cables are attached to lifting yokes at some height above the beam's centroid. The yokes are in turn attached to the beam, not necessarily at its ends (Fig. 5(c)). The yokes can be inclined at any angle, but are usually either fixed to be vertical or allowed to rotate in line with the cables.

Previous work

13. There has been some previous work on the stability of concrete beams. Swann and Godden[14] investigated the lateral buckling of concrete beams lifted by cables and presented a

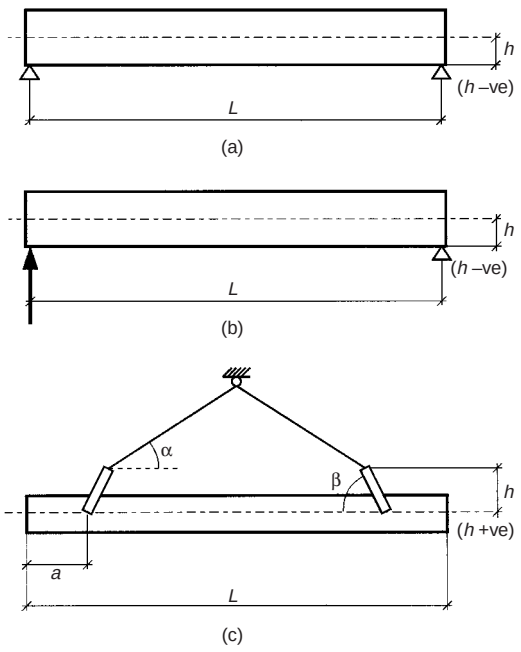

Fig. 5. The three support conditions for beams considered in this paper: (a) simply supported at both ends; (b) supported as for transportation, with the left-hand end supported against displacement, but not rotation; (c) hanging from cables at an angle α, with yokes at angle β (in practice, β will be either α or 90°)

numerical method for determining how they behave. Baker and Edwards[15] gave a method for analysing the non-linear behaviour of thin-walled reinforced and prestressed beams which might be used to analyse the stability of all three support conditions. However, in both cases the analysis is complicated and neither paper leads to a simple design formula. Anderson[16] and Mast[17,18] gave a simple analysis for some special cases. That analysis differs from the present study, since the beam was assumed to have rotational restraint at both supports, provided by springs, the stiffness of which was determined by the vehicle's suspension. A simple test on a lorry in the UK showed that its suspension is an order of magnitude stiffer than that found in the USA by Mast. An extensive analysis of the stability problem by Lebelle[19] uses infinite series to define the buckling shape of the beam, and does not simplify the hanging-beam problem, as will be done here, by separating the torsional and lateral displacement components. A simplified extract from his analysis is presented by Leonhardt.[20] There is also some work available in German[21–23] but this is limited in extent and difficult to obtain. Hansell and Winter[24] and Siev[25] have studied the problems associated with loss of stiffness due to cracking in reinforced concrete beams, but that is not relevant to the present work.

Beam parameters

14. The parameters used to define the models (shown in Fig. 5) are

- the length of the beam L
- the material and section properties: the Young's modulus E, the shear modulus G, the second moment of area about the major axis I_x, the second moment of area about the minor axis I_y, the St Venant's torsion constant J, the warping constant Γ, the distance of the shear centre below the beam's centroid y_{sc} and the height of the centroid above the beam soffit y_b
- the height of the support h, measured positive upwards from the beam centroid (When simply supported or transport-supported, the beam generally rests on its bottom flange, and hence the support height $h = -y_b$. During lifting this dimension is determined by the arrangement of the lifting yokes.)
- the self-weight of the beam w per unit length.

In addition, for a hanging beam, the parameters include

- the distance of the support positions from the end of the beam, a
- the angle of the lifting cables above the horizontal, α, and the angle of the yokes to the horizontal, β.

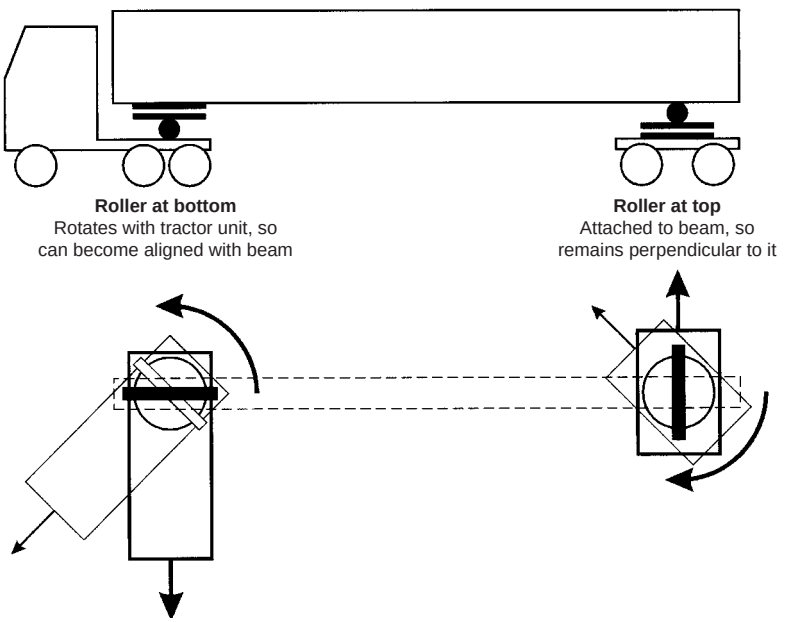

Fig. 6. Details of the supports provided by a tractor unit and trailer during transportation of a beam (note the different arrangement of turntable and roller at the two ends, and the possibility of loss of rotational stiffness at the tractor end)

Warping restraint

15. Warping is the axial distortion of a section due to torsion,[26] and is governed by the magnitude of the warping constant Γ, which has units of L^6. This should be considered for thin-walled sections (such as steel I-beams) since restraint of this deformation effectively increases the stiffness of a beam, and hence its buckling load. The effects of beam warping were investigated in a preliminary study,[27] where it was found that for a typical concrete beam section the effects of warping restraint are negligible. The parameter $\sqrt{(E\Gamma/GJ)}$ (which has units of length) is small compared to the depth of the beam, which indicates that restrained warping effects are negligible. Thus, in the results that follow, no account has been taken of warping effects.

Properties of material and section

16. Most of the results presented below are expressed in non-dimensional form so they can be applied to a variety of cross-sections. However, certain illustrative calculations are given for the largest beam in the SY series, the SY-6,[4] which is designed for spans of up to 40 m. The relevant section properties are given in Table 1. The elastic moduli have been taken as $E = 34\ \text{kN/mm}^2$ and $G = 14{\cdot}2\ \text{kN/mm}^2$, which are typical of the short-term values for concrete in precast beams; since buckling is essentially a short-term phenomenon, no allowance needs to be made for creep effects.

Finite-element analysis

17. Owing to the complexity of the stability analyses for the three different support conditions, not all of which are amenable to analytical solution, finite-element methods have been used to produce the design charts.

Two separate finite-element analyses were performed.

- An eigenvalue analysis. A simple linear elastic model was set up for a perfect structure. An eigenvalue calculation within the finite-element package allows the critical loads and mode shapes to be determined, but does not, by itself, allow the imperfection sensitivity to be considered.
- A non-linear analysis. A finite-element model was set up which could follow geometric non-linearities. The structure could be given some initial imperfection and the complete load–deflection response produced. This could not give the buckling load but could allow the form and magnitude of the initial imperfection to be varied. This, in turn, allowed the growth of the minor-axis displacements to be determined so that the stresses thereby induced could be calculated. The material was assumed to remain linearly elastic. No account was taken of cracking, since prevention of such cracking would almost certainly be made a limit state for design.

18. The finite-element models were constructed from two-noded, linear beam elements aligned with the beam centroid; these elements were able to allow the effects of warping and the position of the shear centre to be taken into account, although, as indicated above, such effects were not found to be significant. A study of the number of elements needed for reliable results was undertaken;[27] all the results presented here have been obtained from a model with 40 elements evenly distributed along the beam length. The support positions were separated from the centroid by rigid elements.

Buckling-load analysis

19. For all three support conditions, failure may occur by elastic buckling of the beam under its own self-weight. The critical load w_{cr} is defined as the self-weight which causes buckling of a perfect beam. This can be compared with the actual value of the beam's self-weight w.

20. Parametric studies were carried out using the eigenvalue finite-element analysis. These investigated the variation in buckling load with the parameters a, α, h, L, EI_y and GJ.

Simply supported beam

21. It was found that for typical concrete beam sections the non-dimensional buckling load of a simply supported beam is

$$w_{cr} = 28{\cdot}5\frac{\sqrt{(GJEI_y)}}{L^3} \tag{1}$$

This agrees closely with the results quoted by Trahair,[6,7] who derives expressions of the form

Table 1. Properties of beam section

	Symbol	Value for SY-6 beam
Overall beam height: m	d	2
Height of centroid above soffit: m	y_b	0·855*
Distance of shear centre below centroid: m	y_{sc}	0·035‡
Cross-sectional area: m^2	A	0·709*
Second moment of area about major axis: m^4	I_x	0·2837*
Second moment of area about minor axis: m^4	I_y	0·0140†
St Venant's torsion constant: m^4	J	0·0221‡
Warping constant: m^6	Γ	0·00343‡
Self-weight: kN/m	w	16·74*

* From reference 26.
† From simple hand analysis.
‡ From computer analysis.

$$w_{cr} = k\frac{\pi}{L^3}\sqrt{\left[EI_y\left(GJ + E\Gamma\frac{\pi^2}{L^2}\right)\right]} \tag{2}$$

where k depends on the support condition.

22. For a simply supported beam $k = 9{\cdot}04$, and if warping effects are insignificant (as applies here), then Trahair's results give

$$w_{cr} = 28{\cdot}4\frac{\sqrt{(GJEI_y)}}{L^3} \tag{3}$$

The buckling load is independent of the support height h since axial rotation is restrained over the supports.

Transport-supported beam

23. For the transport support condition it was found that the non-dimensional buckling load is

$$w_{cr} = 16{\cdot}9\frac{\sqrt{(GJEI_y)}}{L^3} \tag{4}$$

The finite-element analysis showed this to be independent of the support height h, despite the fact that the end support on a ball does not prevent rotation.

Hanging beam

24. The finite-element analysis showed that the buckling load of a hanging beam is independent of the torsional stiffness GJ, and consequently can be non-dimensionalized using the parameter EI_y/L^3. This is confirmed by the mode shape, which, although it involves a rigid-body rotation, demonstrates only a small *variation* in twist along the beam.

25. Figure 7 shows the variation of the non-dimensional buckling load with the geometry of the beam. Each plot is for a different value of the cable angle α and shows curves for different non-dimensional support heights h/L. These give the variation in buckling load with the non-dimensional attachment position a/L. (Note the different scales used for the load axis on each plot.)

26. Similar results have been presented for steel beams by Dux and Kitipornchai,[9] although for these the buckling modes include torsional effects. The wide flanges and thin web of a typical steel beam give it a ratio of torsional to lateral stiffness that is more than an order of magnitude smaller than for a concrete beam. (For example, a steel 914 × 419 × 388 kg/m UB beam has $GJ/EI_y = 0{\cdot}014$, while a concrete SY-6 beam has $GJ/EI_y = 0{\cdot}66$.) In consequence, for steel beams, the torsional component of lateral–torsional buckling is important.

27. The graphs in Fig. 7 show that the buckling load increases with the support height, as the cables approach vertical, and as the yoke attachment points approach the beam's quarter points ($a/L = 0{\cdot}25$). The peak in the buckling load at the beam's quarter points is due to the changing mode shape as the support position is changed.

28. Owing to the arrangement of prestress in the beam, it is not normally possible to support a beam very far from its ends (and certainly not at the quarter points). End support corresponds to the most critical case for buckling and so additional plots are given in Fig. 8 showing the buckling loads for beams supported at $a/L < 0{\cdot}1$.

29. These plots are intended for use as design charts, and their use in this way will be considered in the companion paper.[12]

30. Figure 9 shows the twist component of the buckling modes for an end-supported hanging beam, normalized by the largest twist. It shows that the variation in twist is very small. The buckling of a hanging beam can thus be idealized as a rigid-body rotation about the bottom of the cables, together with a minor-axis buckle; this will be referred to as toppling. Such a geometry can be studied analytically; the results of such a study are presented elsewhere.[28] The equations that result are complex, but can be solved relatively easily using, for example, the solver in a spreadsheet. Cases which are not covered by the charts in Fig. 8 can be solved using the results of that study. For the cases covered by Fig. 8, the analytical solution, despite the simplification caused by ignoring twist, gives results which are only fractionally different from the finite-element results.

Comparison of buckling loads for different support conditions

31. Table 2 gives values of the buckling load w_{cr} for a 40 m long SY-6 beam subject to various support conditions and compares these values to the beam's self-weight w using the parameter w/w_{cr}. The buckling load for a hanging beam is much smaller than that for a simply supported or transport-supported beam. This is due to the lack of torsional restraint about the beam's axis, allowing it to rotate until

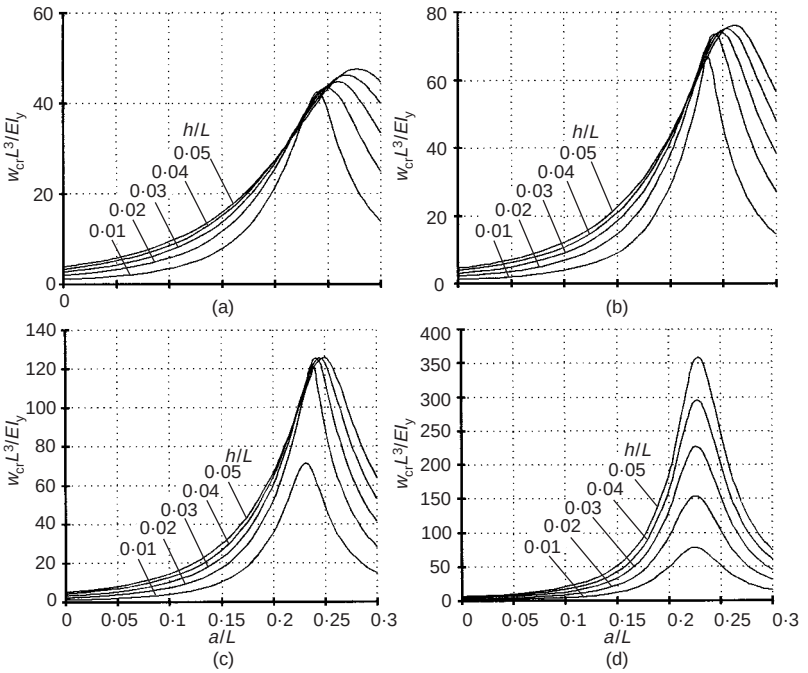

Fig. 7. Critical self-weight loads for hanging beams, for vertical yokes ($\beta = 90°$), obtained using finite-element analyses. For different cable angles α: (a) $\alpha = 30°$; (b) $\alpha = 45°$; (c) $\alpha = 60°$; (d) $\alpha = 90°$. The values of a/L and h/L correspond to the various support configurations (Fig. 5) (note the different scales on the vertical axes)

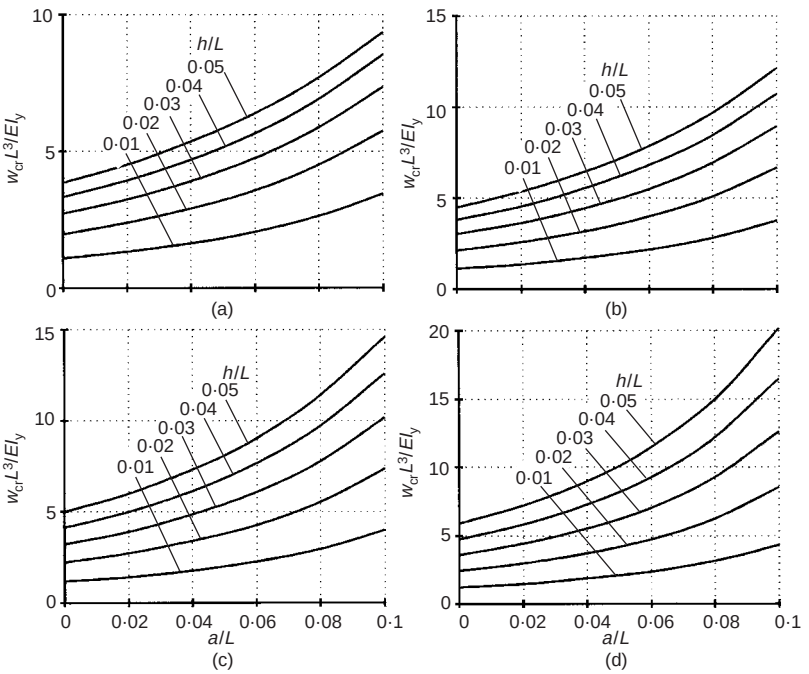

Fig. 8. Design charts for determining the buckling load of a hanging beam supported close to its ends (enlarged views of Fig. 7; (a)–(d) as in Fig. 7). (a) $\alpha = 30°$; (b) $\alpha = 45°$; (c) $\alpha = 60°$; (d) $\alpha = 90°$

it finds an equilibrium position. A hanging beam is thus considerably more likely to buckle than a simply supported or transport-supported beam. This support condition should be given careful consideration when handling a beam.

Initial-imperfection analyses

32. The buckling-load analyses described above are interesting in their own right. However, problems can arise even if the beam's weight is less than the buckling load, but is still a significant fraction of it. In these circumstances an initial imperfection can grow as the load is applied, which can lead to unacceptable stresses before buckling occurs.

33. Non-linear finite-element models were constructed to establish the sensitivity of each support condition to initial imperfections. The load–deflection behaviour of the beam was investigated by varying its self-weight.

The Southwell plot

34. A Southwell plot can be used to represent the load–deflection behaviour of a beam that is approaching its buckling load. It is primarily used as an experimental tool, since it allows an accurate estimate to be made of the actual buckling load even if a well-defined buckle is masked by initial imperfections. It will be used in a different way here, although the underlying analysis remains the same.

35. Southwell[29] showed that a plot of deflection/load against deflection for a neutrally stable flexural buckling problem became asymptotic to a straight line. This line has a gradient of 1/(critical load) and an intercept on the deflection axis of $-v_0$, where v_0 is the component of the initial imperfection in the buckling mode, as shown in Fig. 10(a). It should be noted that the deflection that has to be plotted is the one measured from the initial position of the *imperfect* beam ($v - v_0$), and not that measured from the axis of the *perfect* beam (v). In an experimental set-up, the magnitude of the initial imperfection often cannot be measured directly, and has to be inferred from the Southwell plot.

36. The Southwell construction can also be used in reverse to predict the load–deflection behaviour of a neutrally stable flexural buckling problem given only values of the critical load and the magnitude of the initial imperfection, as shown in Fig. 11(b). The deflection v due to a given self-weight w can be obtained from

$$v = \frac{v_0}{1 - w/w_{cr}} \qquad (5)$$

37. It has been shown that the hanging beam buckles about the beam's minor axis and is hence a flexural buckling problem. Equation (5) thus applies to the hanging-beam case.

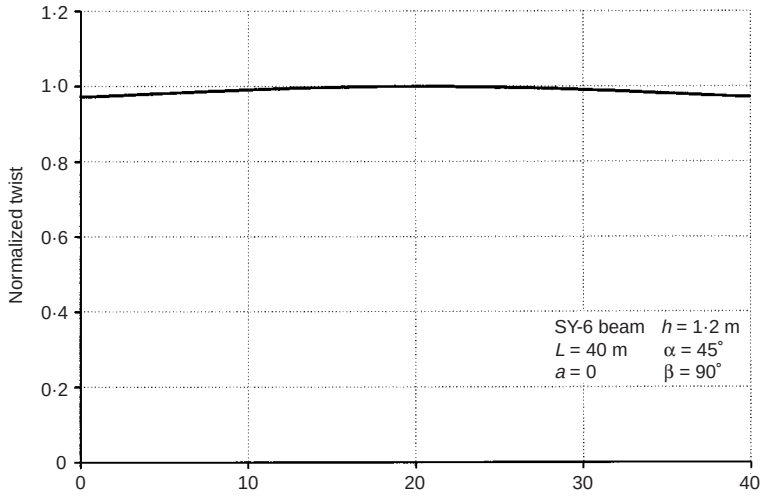

Fig. 9. The twist component of the buckling mode of a hanging beam

*Table 2. Values of buckling load for 40 m long beam**

SY-6 beam	Buckling load w_{cr}: (kN/m)	w/w_{cr}
Simply supported	172	0·10
Transport supported	102	0·16
Hanging, $\alpha = 90°$	34·9	0·48
Hanging, $\alpha = 45°$	28·1	0·60
Self-weight	16·7	

*For the hanging beams, $h = 1{\cdot}6$ m and $a = 0$.

However, both the transport-supported and the simply supported beam buckle in a lateral–torsional manner. Allen and Bulson[8] (for example) show that the lateral deflection of a beam under lateral–torsional buckling should be represented in the form

$$y = \frac{y_0}{1 - (w/w_{cr})^2} \qquad (6)$$

Thus it is appropriate to construct a modified Southwell plot in which deflection/(load)^2 is plotted against deflection, giving a line with gradient of 1/(critical load)^2 and an intercept on the deflection axis of $-y_0$.

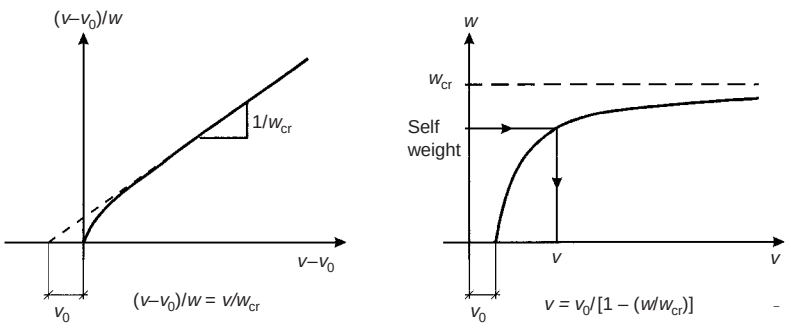

Fig. 10. (a) Southwell plot showing linear behaviour as the load approaches its critical value; (b) corresponding load–deflection plot

38. The load–deflection behaviour, obtained in the present work from initial-imperfection finite-element analyses, can be compared with the behaviour predicted using Southwell plots, constructed using the buckling load given by the eigenvalue finite-element analyses. If this is shown to give a good correlation, the way is clear for a simple hand technique which obtains the critical load from the design charts and the initial imperfections from measurements on site.

Initial lateral bow

39. The first initial imperfection investigated was a lateral parabolic bow. This would typically result from variations in the force in the prestressing tendons, which cause the beam to deflect to one side.

Simply supported and transport-supported beams

40. Figure 11 shows load–deflection and modified Southwell plots for an SY-6 beam simply supported over a span of 40 m, containing an initial lateral imperfection of magnitude 50 mm, which is about twice as large as typical measured imperfections for such beams. The plots use the non-dimensional parameters midspan deflection $= (y_{ms} - \delta_0)/L$ and load $= wL^3/\sqrt{(GJEI_y)}$ (y_{ms} is the lateral deflection of the beam at midspan, measured relative to the supports along a fixed axis, and δ_0 is the magnitude of the initial imperfection at midspan). The dashed lines are constructed using equation (6) and values of the critical load obtained from the eigenvalue finite-element analysis, while the solid lines are from the non-linear finite-element analysis.

41. The modified Southwell plot shows the non-linear finite-element analysis to be asymptotic to the line predicted using equation (6), although a small discrepancy between the gradients of the lines is apparent. However, the modified Southwell construction is conservative and hence can be used to determine the expected lateral deflection of a beam.

42. It is the *stresses* in the concrete, rather than the deflection, that will cause failure of the beam. These, in turn, are due to curvature. To assess the curvature of the simply supported or transport-supported beam, it is necessary to determine the buckled shape. The Rayleigh–Ritz method,[8,30] based on an assumed approximation to the buckling mode, can be used to give an upper-bound solution for the buckling load. By minimizing the buckling load, a close approximation to the buckled shape can be determined which will be sufficiently accurate for the present purposes.

43. For the simply supported beam, assuming a simple sinusoidal mode shape in both the lateral deflection and the twist gives a buckling load within 2% of that given in equation (1). The relative magnitudes of the twist and the lateral deflection are then related by

$$\frac{\delta\theta}{y} = \frac{\pi}{L}\sqrt{\left(\frac{EI_y}{GJ}\right)} \tag{7}$$

44. For the transport-supported beam, one support allows rotation, which is allowed for by assuming a mode shape of the form

$$y = A_1 \sin\frac{\pi x}{L} - A_3 y_b \frac{x}{L}$$
$$\delta\theta = A_2 \sin\frac{\pi x}{L} + A_3 \frac{x}{L} \tag{8}$$

where y_b is the height of the shear centre above the centroid, which will be close to the centroid for most concrete beams.

45. If appropriate values for the constants A_1 to A_3 are chosen, this mode shape gives a buckling load within 4% of that given by equation (4). The relative magnitudes of the twist and midspan lateral deflection are then given by

$$\frac{\delta\theta}{y_{ms}} = \frac{1{\cdot}68}{-0{\cdot}36L\sqrt{(GJ/EI_y)} - y_b} \tag{9}$$

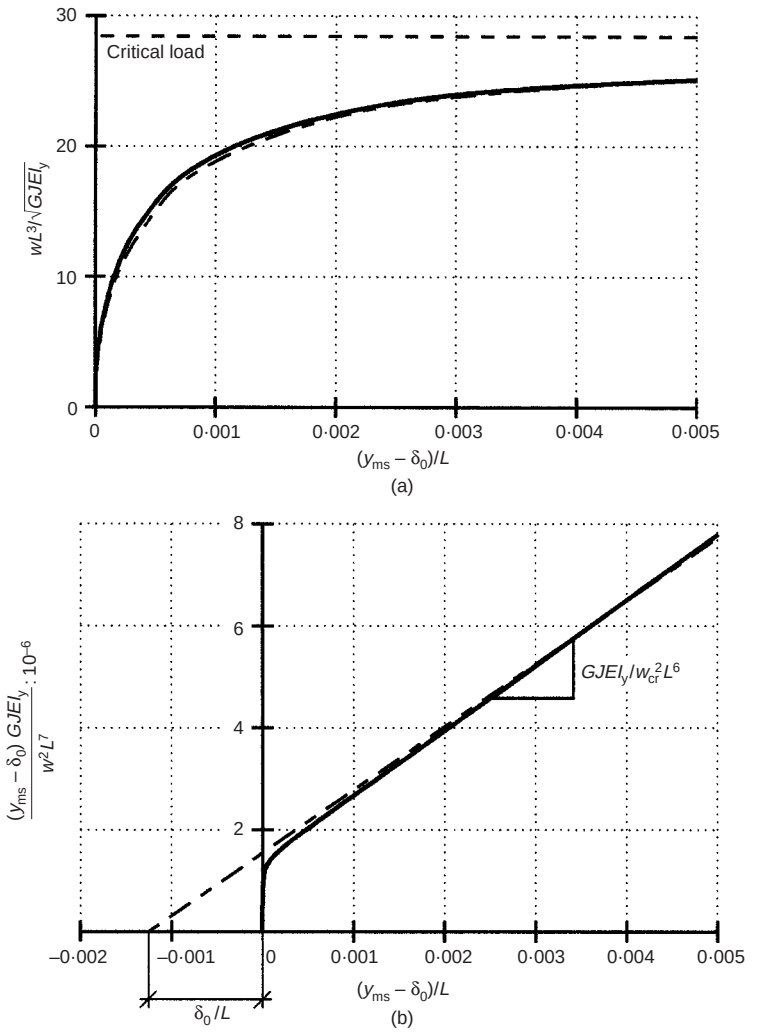

Fig. 11. (a) Load–deflection behaviour and (b) modified Southwell plot for a simply supported beam with an initial lateral bow of δ_0 = 50 mm (solid lines, non-linear finite-element analysis; dashed lines, constructed from equation (6))

The minor-axis bending moment in a simply supported or transport-supported beam at midspan can then be found from equilibrium; the self-weight bending moment about a horizontal axis is $wL^2/8$, so the minor-axis component is $wL^2 \sin\delta\theta/8$.

46. Thus, the maximum lateral curvature for a simply supported or transport-supported beam occurs at midspan and is given by

$$\kappa_{ms} = \frac{wL^2 \sin\delta\theta}{8EI_y} \tag{10}$$

Hanging beam

47. Figure 12 shows load-deflection and Southwell plots for a typical hanging beam, with an initial imperfection of magnitude 100 mm. (This is an extreme value for an initial imperfection, chosen for the purposes of illustration. A more typical initial imperfection size might be 30 mm.) Since a hanging beam buckles laterally, the deflection parameter v_{ms} is used. This is measured along the minor axis of the beam, which rotates with the rigid-body motion.

48. The plots show that a hanging beam buckles in a stable manner, the load capacity continues to increase as the deflection gets larger (this is discussed in more detail elsewhere[28]). The post-buckling behaviour is positively stable (rather than neutrally stable), which means that the results from the non-linear analysis are not asymptotic to the predictions of the Southwell construction. However, the predictions of the Southwell construction (which are easy to determine) are a good approximation to the accurate load–deflection response (which is very difficult to calculate) up to about $w = 0{\cdot}7w_{cr}$ and are conservative in that they overestimate the associated deflection, and hence curvature. They can thus be used as a basis for the calculation of curvatures and stresses.

49. The correct initial imperfection for use in the Southwell construction is measured from the support positions. Assuming a sinusoidal initial imperfection, this is given by $\delta_0(1 - \sin(\pi a/L))$. Hence, from equation (5)

$$v_{ms} = \frac{\delta_0(1 - \sin(\pi a/L))}{(1 - w/w_{cr})} \tag{11}$$

In the same way, the midspan curvature, which for a sinusoidal imperfection is given by $-\pi^2\delta_0/L^2$, will also be magnified by the same factor $1/(1 - w/w_{cr})$. A more accurate value for the curvature can be found from equations given elsewhere.[28]

Initial support rotation

50. The second initial-imperfection analysis investigated the effect of placing a simply supported or transport-supported beam on sup-

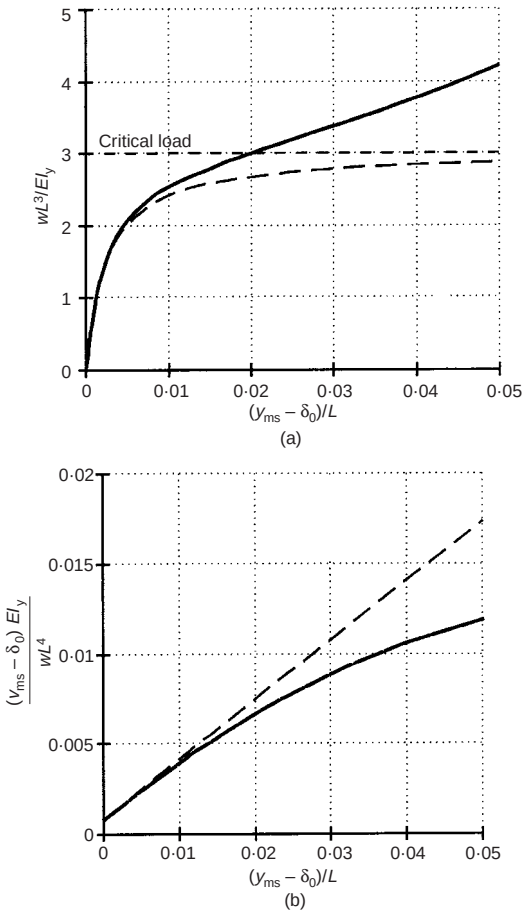

Fig. 12. (a) Load–deflection behaviour and (b) Southwell plot for a hanging beam with an initial lateral bow of δ_0 = 100 mm (solid lines, non-linear finite-element analysis; dashed lines, Southwell prediction from eigenvalue analysis)

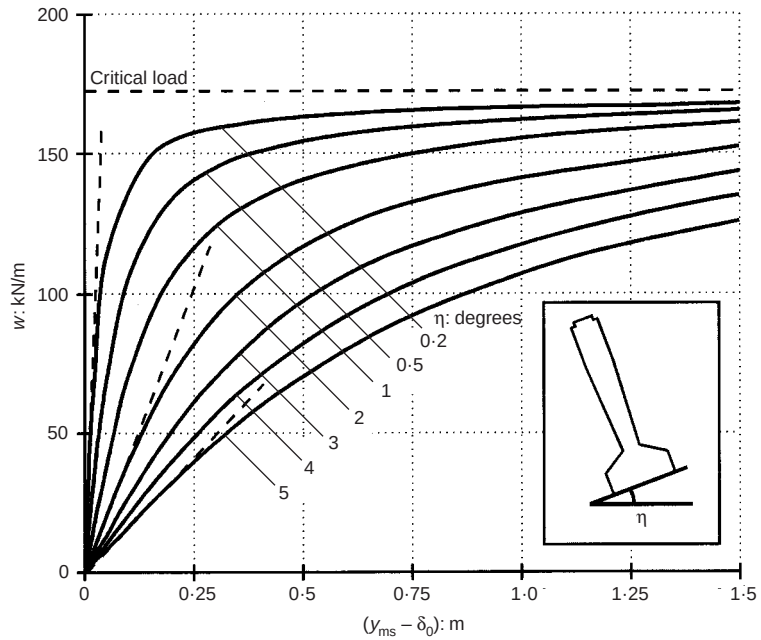

Fig. 13. Load–deflection behaviour of a simply supported beam resting on inclined supports

ports which are not level. The beam is thus initially tilted (as shown in Fig. 13), where the angle of the supports from the horizontal is η. For the simply supported case this might occur during erection and jacking, or because of a combination of bearing flexibility and imperfect placement. During transportation, road camber would give an angled support—a typical road camber in the UK is about 3°, but cambers of 6° could be encountered, and larger rotations can be envisaged on site.

51. Figure 13 shows a load–deflection plot for a 40 m long SY-6 beam, simply supported on inclined supports, for various support angles; these responses have been obtained from the non-linear finite-element analysis. As already discussed, the simply supported beam buckles in a lateral–torsional manner, involving both minor-axis displacement and twist about the beam's axis. However, for small loads (approximately $w < w_{cr}/4$) the torsional effects are negligible, and the lateral deflection of the beam is due to the component of the load which acts in the minor-axis direction ($w \sin \eta$). The midspan minor-axis deflection y_{ms} is found by assuming that the beam is simply supported for minor-axis bending, so that

$$y_{ms} - \delta_0 = \frac{5wL^4 \sin \eta}{384EI_y} \tag{12}$$

The midspan deflection thus increases linearly with the beam's self-weight for small loads. This is indicated by the dashed lines in Fig. 13.

52. Figure 14 shows modified Southwell plots for the same beam at various support angles. These tend towards lines with gradient $1/w_{cr}^2$. They are clearly asymptotic to the same critical load.

53. By extrapolating the straight portion of these plots (as in Fig. 11) the apparent initial imperfection (δ_0) can be determined. It would be convenient if δ_0 could be predicted from the initial support rotation η since this would allow the load–deflection curve to be determined without recourse to complex analysis. However, Fig. 14 shows this not to be the case. The value of δ_0 increases with η, but not uniformly.

54. It might be suspected that the initial imperfection could be established by evaluating the lateral deflection of the beam due to the component of the load acting in the minor-axis direction, from equation (12). Figure 14(b) shows lines corresponding to this relationship for $w = 16{\cdot}7$ kN/m (the self-weight of an SY-6 beam) and $w = w_{cr} = 172$ kN/m (the buckling load of the simply supported beam). The correct initial imperfection lies between the two, but there is no easy way of establishing this for a particular beam, owing to the lateral torsional behaviour of the beam. This is not particularly

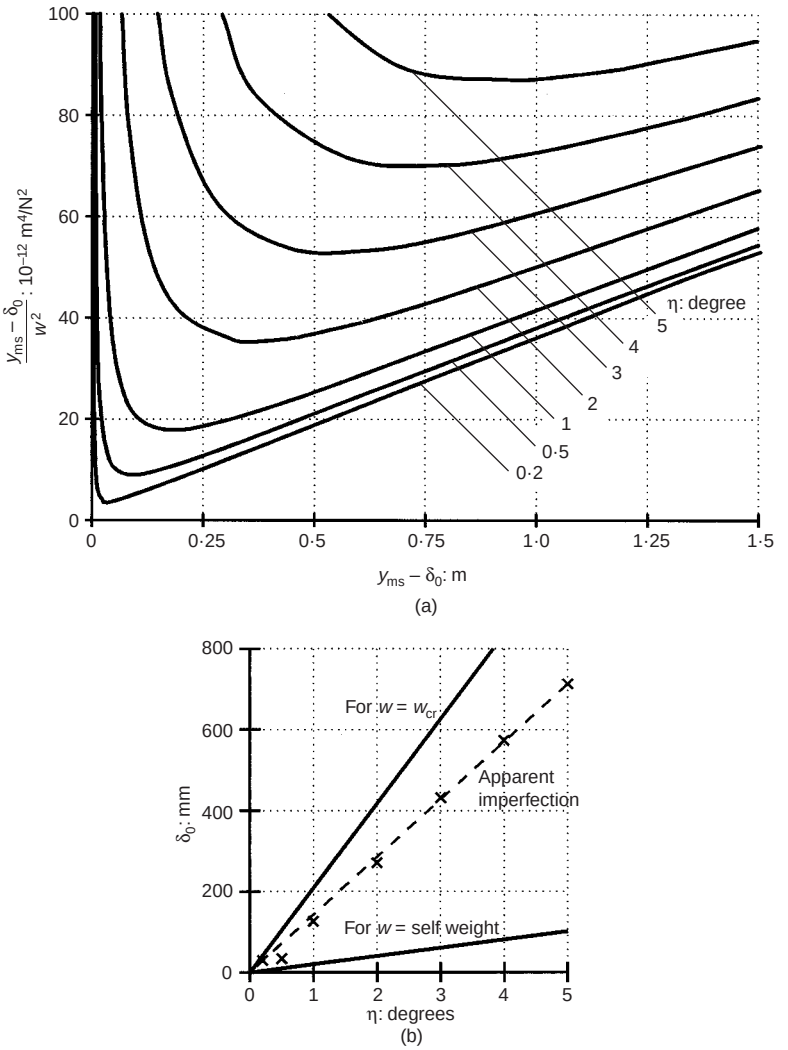

Fig. 14. (a) Modified Southwell construction for a simply supported beam resting on inclined supports; (b) see text

surprising, since the value of δ_0 is the component of the initial imperfection mode, and should be independent of the load on the structure. By assuming that the initial deflection is itself a function of the beam's load, that independence is lost, and no simple relationship should be expected.

55. All is not lost, however. It has been shown that the buckling load of a hanging beam is much lower than that of a simply supported beam. For a beam to be lifted it must therefore have a self-weight which is considerably less than the critical load shown in Fig. 13, and it will be reasonable to use equation (12) to predict the deflection when a beam is placed on inclined supports, which avoids the need to evaluate δ_0.

56. As already discussed, the curvature must be evaluated to determine whether a beam is likely to fail because of excessive stress in the concrete. The maximum minor-axis curvature is given by

$$\kappa_{ms} = \frac{wL^2 \sin \eta}{8EI_y} \tag{13}$$

57. These results show that a simply supported beam is susceptible to inclined supports, and that for self-weights that are small in comparison with the buckling load, the deflection and stresses in the beam can be evaluated in a simple manner. The same logic can be applied to a transport-supported beam.

Conclusions

58. The behaviour of precast concrete beams may be susceptible to lateral or lateral–torsional buckling under self-weight conditions before the beams are stabilized by inclusion in a structure. It has been shown that there are three principal cases which need to be considered: the hanging beam, the transport-supported beam and the simply supported beam. Of these, it has been shown that the hanging beam is the most critical case since no restraint is provided against rigid-body rotation.

59. It has been shown that a simple analysis of the critical load can be combined with a Southwell plot analysis to allow the effects of initial imperfections to be investigated.

60. The results presented here are suitable for use in design, using methods that will be described elsewhere.[12]

Acknowledgements

61. The authors would like to thank Dr H. P. J. Taylor of Tarmac Precast Concrete Limited, and the Prestressed Concrete Association for their help with this project.

References

1. Somerville G. *Standard Bridge Beams for Spans from 7 m to 36 m*. Cement and Concrete Association, London, 1970.
2. Manton B. H. and Wilson C. B. *MoT/C&CA Standard Bridge Beams, Prestressed Inverted T-beams for Spans from 15 m to 29 m*. Cement and Concrete Association, London, 1971.
3. Taylor H. P. J., Clark L. A. and Banks C. C. The Y-beam: a replacement for the M-beam in beam and slab bridges. *The Structural Engineer*, 1990, **68**, 459–465.
4. Prestressed Concrete Association. *Data Sheet for SY-beams*. Prestressed Concrete Association, Leicester, 1995.
5. Laszlo G. and Imper R. R. Handling and shipping of long span bridge beams. *PCI Journal*, 1987, **32**, 86–101.
6. Trahair N. S. *The Behaviour and Design of Steel Structures*. Chapman and Hall, London, 1977.
7. Trahair N. S. *Flexural–Torsional Buckling of Structures*. E. & F. N. Spon, London, 1993.
8. Allen H. G. and Bulson P. S. *Background to Buckling*. McGraw-Hill, London, 1980.
9. Dux P. F. and Kitipornchai S. Stability of I-beams under self-weight lifting. *Steel Construction—Journal of the Australian Institute of Steel Construction*, 1989, **23**, No. 2, 2–11.
10. Parker D., Bolton A. and Cruickshank J. Bernay beam failure rocks French engineers. *New Civil Engineer*, 7 Oct. 1993, 3–5.
11. New Civil Engineer. Poor support blamed for bridge tragedy. *New Civil Engineer*, 28 Apr. 1994, 4.
12. Stratford T. J., Burgoyne C. J. and Taylor H. P. J. Stability design of long precast concrete beams. *Proceedings of the Institution of Civil Engineers: Structures and Buildings*, 1999, **134**, 159–168.
13. Burgoyne C. J. and Stratford T. J. Buckling of heavy beams on rotationally flexible bearings. *The Structual Engineer*, submitted.
14. Swann R. A. and Godden W. G. The lateral buckling of concrete beams lifted by cables. *The Structural Engineer*, 1966, **44**, 21–33.
15. Baker G. and Edwards A. D. A limit analysis of non-linear elastic displacements of thin-walled reinforced and prestressed beams. *Engineering Structures*, 1985, **7**, 198–203.
16. Anderson A. R. Lateral stability of long prestressed concrete beams. *PCI Journal*, 1971, **16**, 7–9.
17. Mast R. F. Lateral stability of long prestressed concrete beams, part 1. *PCI Journal*, 1989, **34**, 34–53.
18. Mast R. F. Lateral stability of long prestressed concrete beams, part 2. *PCI Journal*, 1993, **38**, 70–88.
19. Lebelle P. Stabilité élastique des poutres en béton précontraint a l'égard de déversement latéral. *Ann. Batiment et des Travaux Publics*, 1959, **141**, 780–830.
20. Leonhardt F. *Prestressed Concrete—Design and Construction* (trans. C. van Amerongen). Ernst & Sohn, Berlin, 1964, 2nd edn.
21. Deneke O., Holz K. and Litzner H. Übersicht über praktische Verfahren zum Nachweis der Kippersicherheit schankler Stahlbeton- und Spannbetonträger (Survey of practical methods of checking the lateral stability of slender reinforced or prestressed concrete beams). *Beton und Stahlbetonbau*, 1985, **80**, No. 9, 238–242.
22. Stiglat K. Zur Näherungsberechnung der Kipplasten von Stahlbeton- und Spannbetonträgern über Vergleichsschlankheiten (Approximate calculation of the lateral stability of reinforced concrete and prestressed concrete beams by means of comparative slenderness values). *Beton und Stahlbetonbau*, 1991, **86**, No. 10, 237–240.
23. König G. and Pauli W. Nachweis der Kippstabilität von schlanken Fertigteilträgern aus Stahlbeton und Spannbeton (Verification procedure of the lateral stability of slender prefabricated and prestressed concrete girders). *Beton und Stahlbetonbau*, 1992, **87**, No. 5, 109–112.
24. Hansell W. and Winter G. Lateral stability of reinforced concrete beams. *Proceedings of the American Concrete Institute*, 1959, **56**, 193–213.
25. Siev A. The lateral buckling of slender reinforced concrete beams. *Magazine of Concrete Research*, 1960, **12**, 155–164.
26. Timoshenko S. P. and Gere J. M. *Theory of Elastic Stability*. McGraw-Hill, New York, 1961, 2nd edn.

27. Stratford T. J. *The Stability of Long Precast Concrete Bridge Beams*. Cambridge University Engineering Department, 1996, Part IIB project report.
28. Stratford T. J. and Burgoyne C. J. The toppling of hanging beams. *International Journal of Solids and Structures*, in press.
29. Southwell R. V. On the analysis of experimental observations in problems of elastic stability. *Proceedings of the Royal Society, London, Series A*, 1932, **135**, 601–616.
30. Bazant Z. P. and Cedolin L. *Stability of Structures*. Oxford University Press, Oxford, 1991.

Please email, fax or post your discussion contributions to the publisher: email: ttjournals@ice.org.uk; Fax: 0171 538 9620; or post to Terri Harding, Journals Department, Thomas Telford Limited, Thomas Telford House, 1 Heron Quay, London E14 4JD.